Plasma Medicine, 8(1):57–71 (2018)

Linear Microdischarge Jet for Microbiological Applications

E. Tyczkowska-Sieroń,[a] R. Kapica,[b] J. Markiewicz,[b] & J. Tyczkowski[b,*]

[a]Department of Environmental Biology, Medical University of Lodz, Poland; [b]Department of Molecular Engineering, Faculty of Process and Environmental Engineering, Lodz University of Technology, Poland

*Address all correspondence to: J. Tyczkowski, Department of Molecular Engineering, Faculty of Process and Environmental Engineering, Lodz University of Technology, Wolczanska 213, 90-924 Lodz, Poland; Tel.: +48 42 631 3723; Fax: 48 42 636 5663, E-mail: jacek.tyczkowski@p.lodz.pl

ABSTRACT: A new type of linear cold atmospheric-pressure plasma source, the plasma razor jet, was devised. Operational parameters, such as the lowest required power for igniting the plasma, the power below which the plasma is extinguished, and the power at which the discharge arc occurs, were determined. Optical emission spectra and the treated surface temperature were also investigated. Based on the diffuse model for linear light sources, the distribution of plasma irradiation was calculated. It was found that the plasma razor jet is well fit for surface treatment, providing sufficiently uniform irradiation during scanning. This device was tested as a cold atmospheric-pressure plasma source for treatment of pathogenic fungi, such as *Candida albicans* and *Prototheca zopfii*. To compare the effectiveness of the plasma in eradicating various microorganisms, the concept of minimal lethal dose (D_{min}) is introduced.

KEY WORDS: cold atmospheric-pressure plasma, linear plasma source, pathogen fungi, minimal lethal dose

I. INTRODUCTION

Since the mid-1990s, when nonthermal atmospheric-pressure plasma began to be used in biomedical technology, we have been witnessing the rapid development of this field.[1,2,3] Many atmospheric-pressure plasma sources have been constructed. Among these are sources generating nonthermal (cold) plasma, very often in the form of plasma jets and plasma needles, which are particularly suited to medical and biological applications.[4,5,6,7,8,9,10] In general, these plasma sources are small in size and generate plasma in the shape of a ball with a diameter of a few millimeters, or they are in the shape of a plum of with a diameter of a few millimeters and a length of several centimeters. Such plasma volume is beneficial for precise operations but is insufficient for treating larger surfaces.

Large-area or large-linear cold atmospheric-pressure plasma sources are a difficult challenge, particularly with regard to stringent biomedical demands for processing reproducibility in the face of great variation in sample materials and their surface topology.[11] A number of designs have been proposed, but as yet none are universally applicable. One such large-volume design comprises multineedle plasma at atmospheric pressure stabilized by the flow of a working gas through a high-voltage electrode operated by

an AC (20-kHz) power supply.[12] Nie et al.[11] designed a scalable two-dimensional (2D) array of seven cold atmospheric-pressure plasma jets in a honeycomb configuration. Lee et al.[13] devised a multijet system where the power electrode is composed of 500 hollow cathodes with inner diameters of 0.5 mm. In Choe et al.'s[14,15] system, an atmospheric large-volume (200 × 50 × 4 mm^3) glow plasma is generated via the dielectric barrier discharge (DBD) method. The drawback of this system is the relatively high plasma gas temperature, approximately 490–630 K.

Linear plasma sources are based primarily on dielectric-barrier discharge (DBD), where a narrow linear gap in one of the electrodes,[16,17] or simply a linear electrode, such as a quartz tube coated on the inside with aluminum,[18] is used to produce plasma in the form of a thin beam parallel to the substrate. To this end, an ordinary interelectrode discharge in, for example, a magnets-in-motion arrangement with a RF linear hollow cathode system[19] or microplanar RF plasma reactor[20] has been used.

Recently, we devised a linear cold atmospheric-pressure plasma source, the plasma razor jet, which is like the plasma needle except that a razor-shaped linear electrode takes the place of the needle electrode .[21] In this paper, we describe this device, its operation, and its application in the treatment of pathogen fungi.

II. LINEAR MICRODISCHARGE JET

A. Setup Design

The plasma razor jet, shown in Fig. 1, is equipped with a power electrode (1) in the form of a 4.0-cm-long vertical, very thin (0.2 mm) rectangular plate made from stainless steel 316. This electrode is connected to an RF generator (13.56 MHz) through a cable (5). The lower edge of the electrode is sharpened on both sides to form a symmetrical, triangular blade. The entire surface of the electrode, apart from the lower edge, is covered with polytetra-

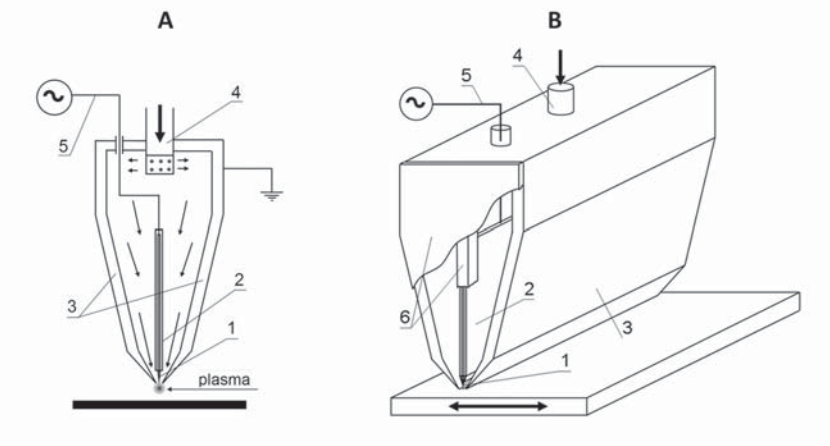

FIG. 1: Plasma razor jet. A: cross-section; B: slant projection

fluoroethylene (PTFE) (2), approximately 0.5 mm thick, to avoid electrical breakdowns and the risk of arc ignition inside the plasma razor chamber. The power electrode is placed using PTFE side plates (6) inside the outer body (3), which is made of stainless steel 316 and serves as a grounded electrode. The distance between the power electrode blade and the lower edges of the grounded outer body (3) is 1 mm on each side. Helium is used as the working gas in the system, either pure or mixed with oxygen, argon, carbon dioxide, and the like. It is supplied by the Swagelok-type connector (4) located centrally on the top of the device and equipped with a diffuser for uniformly dispersing gas inside the chamber.

The cold plasma beam is generated on the lower edge of the power electrode and is shaped like a cylinder with a length equal to the length of the electrode (4 cm) and a diameter of about 1.5 mm. Along the edge, a large electric field gradient is created, which allows the glow microdischarge to be generated in this region at atmospheric pressure using relatively low discharge power.

A schematic view of the experimental system and the working plasma razor jet are shown in Fig. 2. The sample can be treated when stationary by the parallel plasma beam, or it can be scanned by appropriate shifting. Treatment processes are mainly controlled by the discharge power, the working gas composition and flow rate, the distance between the sample surface and the power electrode edge, and the scan procedure.

B. Characteristics of Plasma Razor Jet Operation

1. Operational Power Window

In order to determine the operating conditions for cold atmospheric-pressure plasma sources, the ranges of discharge power and working gas flow rate, in which stable

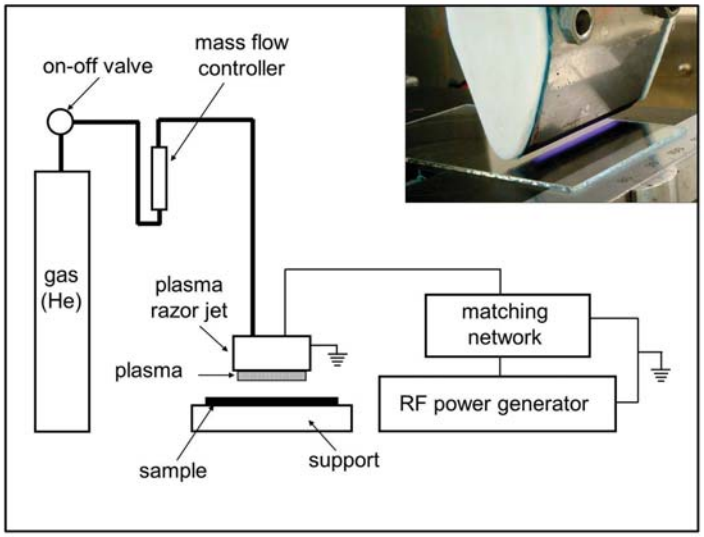

FIG. 2: Schematic of the experimental system (insert: working plasma razor jet)

plasma is produced (operational power window), should be experimentally determined. Figure 3 shows the operational power window for the plasma razor jet used in this study. The lowest required power for igniting the plasma, the power at which the plasma is extinguished, and the power at which the glow discharge turns into arc discharge are presented here as functions of the helium flow rate. It is observed that, as the helium flow rate increases, all three power values initially decrease, reaching constant values above a sufficient high flow rate. This effect is due to the reduction in atmospheric oxygen and nitrogen molecules that diffuse from the surroundings into the plasma region when the helium flow rate increases. The presence of either oxygen or nitrogen (although in very small amounts) increases the ignition power. The mechanism of this increase (breakdown voltage) is different for the two gases: for oxygen, this behavior results from electronegativity; for nitrogen, this behavior is perhaps due to quenching metastable helium upon penning ionization.[22]

2. Optical Emission Spectroscopy

Optical emission spectroscopy was used to characterize the chemical composition of the plasma discharge. Figure 4 shows emission spectra in the range of 200–750 nm, measured by an Ocean Optics HR 4000 spectrometer (with a resolution of 0.3 nm). The main lines were attributed to appropriate atomic and molecular emissions.[23,24] The spectra were recorded for the plasma generated at the same discharge power but at two helium flow rates. One observes, along with the He lines, the oxygen and nitrogen lines, indicating interdiffusion of air into the discharge region. However, the intensity of the

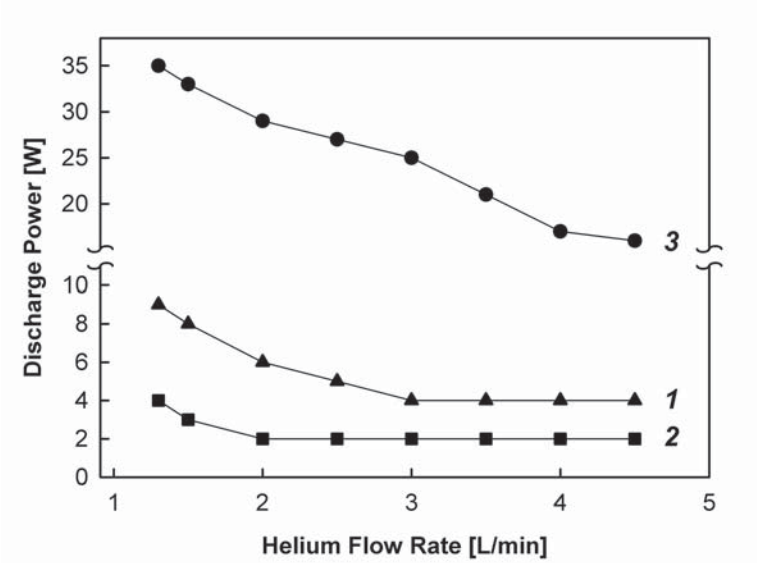

FIG. 3: Operational power window. 1: lowest required power for igniting plasma; 2: power below which plasma extinguished; 3: power at which discharge arc occurs

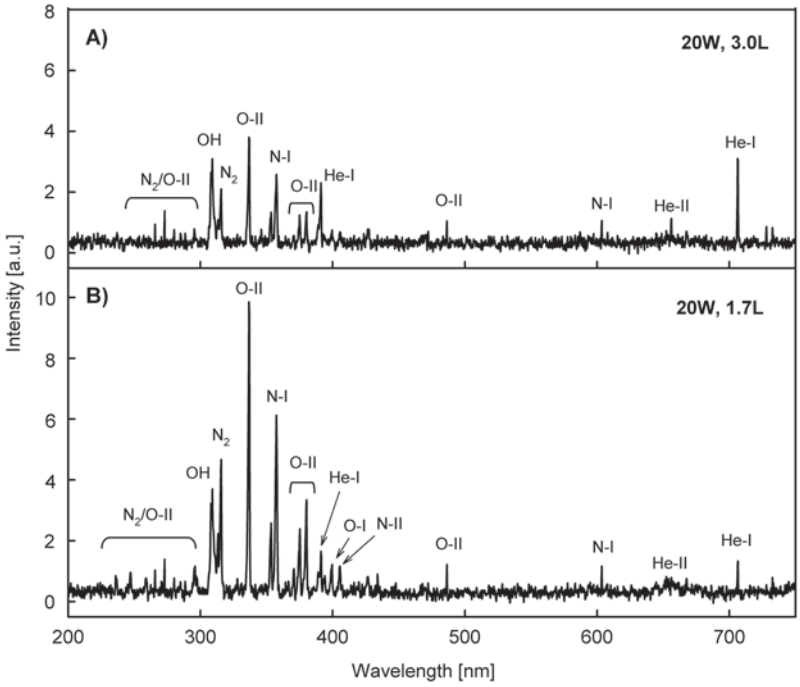

FIG. 4: Optical emission spectra for two helium flow rates

oxygen and nitrogen lines is lower when the helium flow rate is higher. This is in contrast to He line intensity, which increases as the helium flow rate increases, a result that is in good agreement with the aforementioned increase in breakdown voltage when the helium flow rate decreases.

It is important that the composition of the plasma strongly depends on the helium flow rate, even though only pure helium is supplied. Thus, the concentration of free radicals and excited species is controlled by the flow rate parameter. It should also be added that, contrary to general opinion, which says that no significant UV emission occurs in cold atmospheric-pressure plasmas below 285 nm,[1,25,26] we observed some emission lines in this range.

3. Surface Temperature

Before considering the possibility of using the plasma razor jet to treat biological materials, it is necessary to determine how the temperature of the treated surface changes as a result of plasma action. Temperature measurements were performed on the surface of Sabouraud Dextrose Agar (BioMérieux, Marcy-L'Étoile, France) in a Petri dish, in the same experimental system used for further investigations of plasma activity on pathogenic fungi. The plasma razor jet was fixed parallel to the treated surface at a distance

of 5 mm between the surface and the power electrode edge. As a temperature probe, we used a 1-mm-diameter sheathed K-type (NiCr–NiAl) thermocouple connected to a Uni-T UT325 digital thermometer (Uni-T, Dongguan City, Guangdong Province, China) with a fast response time (10 μs) and a resolution of 0.1°C. The thermocouple tip, which goes through the Petri dish from the bottom, was located on the agar surface exactly under the plasma beam at half its length.

Figure 5A shows temperature increase versus time for different flow rates of helium at the same discharge power (17 W). The increases are very small and less than 2°C after the temperature has stabilized. It is interesting, however, that smaller changes in temperature are measured for the higher helium flow rate, which may indicate lower plasma activity due to less diffusion of air into the plasma region. In turn, Fig. 5B shows temperature increase versus time for different discharge power levels at the same helium flow rate (1.9 L/min). The increases are greater for higher power levels, but even in extreme cases do not exceed 20°C, which allows the plasma razor jet to be used for the treatment of biological materials without fear of thermal destruction.

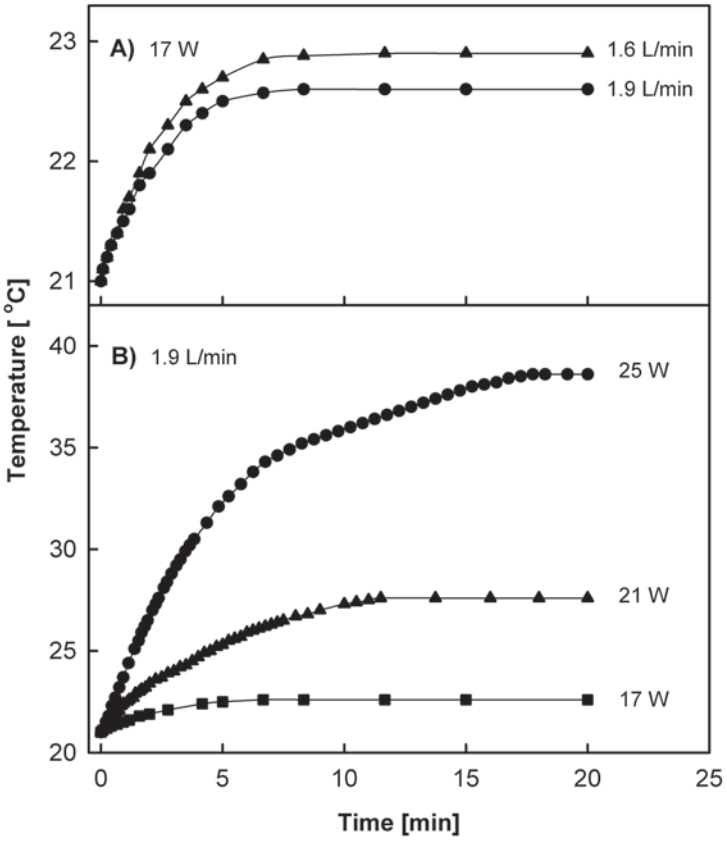

FIG. 5: Temperature changes on medium surface. A: different helium flow rates; B: different discharge power levels

4. Calculation of Plasma Radiation

The so-called five times rule states that the source of radiation can be found as a point radiating isotropically only when the distance between source and detector is at least five times the greatest dimension of the source.[27] Accordingly, our plasma razor jet, with a plasma beam 4 cm long and at a distance to the treated surface of a few millimeters, should be considered a linear source. The plasma beam emits various species, such as free radicals, ions, UV photons, and reactive molecules, all of which act as microbial cell killer agents. By analogy to UV tube lamps, we assume that the total surface irradiation by the killing agents is described by the diffuse model.[28] For the simplest case, the irradiance (E) detected at point P on surface Π_1, on which the linear plasma source is placed (Fig. 6A), can be expressed by[29]

$$E = S_R \left[\frac{L-h}{d\sqrt{d^2+(L-h)^2}} + \frac{h}{d\sqrt{d^2+h^2}} \right] \quad (1)$$

where L is the plasma beam length, S_R is the emission intensity of the killing agents per unit length of the plasma beam, and d and h are, respectively, point P's distance from the linear plasma source and its vertical position.

Taking Eq. (1), we can calculate the irradiance on the surface along line A–B being the vertical projection of the power electrode edge on the surface parallel to this edge (Fig. 6B). This calculation is illustrated in Fig. 7. It should be noted that, in the central part of the razor jet, the plasma radiation is nearly constant. We can use these results to propose the best scan configuration. As one can see in Fig. 8, the most homogeneous irradiance is achieved when the scanning areas border on each other.

To predict the irradiance at any point (P') on the parallel surface Π_2—that is, on the surface treated by the plasma (Fig. 6B)—we can use the following relation:

$$E = S_R \left[\frac{L-h}{\sqrt{d^2+(L-h)^2}} + \frac{h}{\sqrt{d^2+h^2}} \right] \cdot \frac{d^2}{(d^2+c^2)^{3/2}} \quad (2)$$

where c is a distance between line A–B and point P'.

III. MICROBIOLOGICAL APPLICATIONS

A. Materials and Methods

The plasma razor jet was tested as a treatment for pathogenic fungi using the reference strain of *Candida albicans* (ATCC 10231) as well as a selected strain of *Prototheca zopfii* (No XIV).[30] The latter was isolated from milk samples collected in Opole Province, Poland, from cows with clinical or subclinical mastitis in 2015. Two treatment

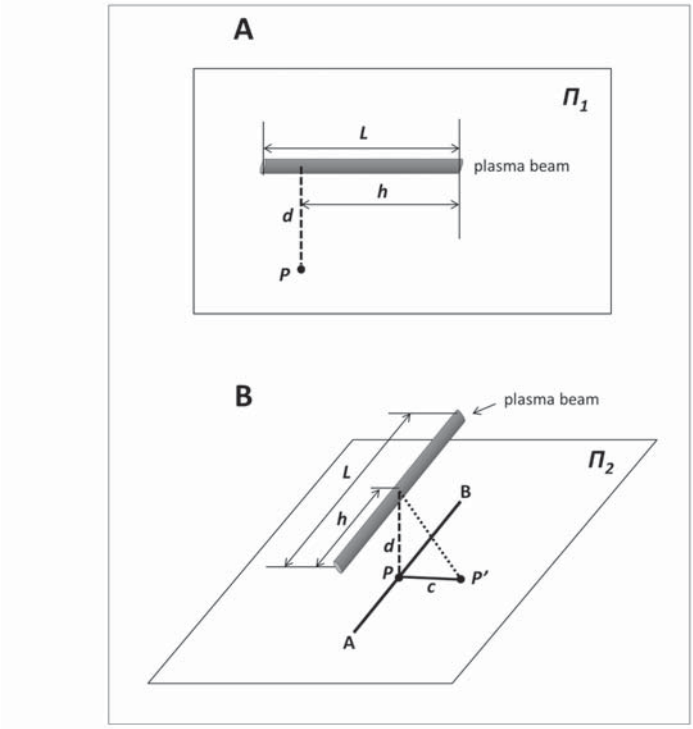

FIG. 6: Schemes for calculating plasma irradiation

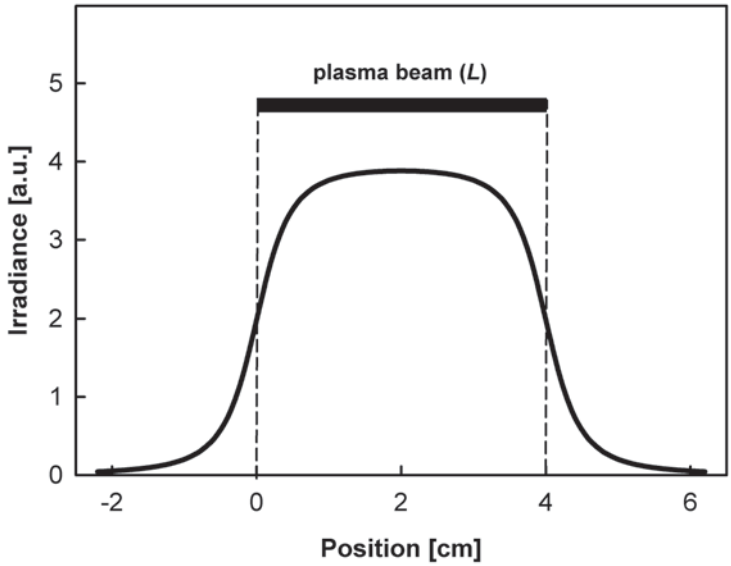

FIG. 7: Distribution of irradiance by plasma on surface along A–B line (see Fig. 6B)

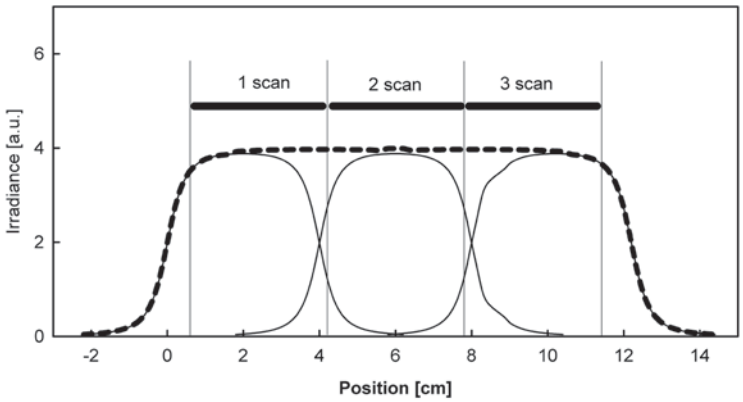

FIG. 8: Calculation of linear plasma source irradiance for scan procedure with scanning areas bordering on each other

procedures were used to determine plasma activity in the interaction with fungal cells. In the first procedure, applied to *C. albicans*, the effect of discharge power and helium flow rate on survival was investigated using very thin films of aqueous fungal cell suspension scanned with the razor jet. Ten microliters of the suspension, containing 5×10^5 CFU/mL were distributed uniformly on an 18 × 18-mm^{2}glass substrate. A film of approximately 30 μm in thickness was thus obtained. The sample with the film was double-scanned by the central part of the plasma razor jet located at a distance of 2 mm and shifted at a rate of 2 mm/s in the transverse direction to the plasma beam. After plasma treatment, the sample was placed in a container containing 1 mL of distilled water and thoroughly shaken. The resulting suspension was quantitatively plated onto a Petri dish with Sabouraud Gentamicin Chloramphenicol 2 Agar (BioMérieux, Marcy-L'Étoile, France**)**, and after 24-h incubation at 37°C colonies were counted. For the same plasma treatment conditions, five independent measurements were taken, the results of which were averaged.

The second procedure, applied to both *C. albicans* and *P. zopfii*, comprised stationary plasma action on the fungi cultures at different treatment times. Each culture was prepared by uniformly spreading 100 μL of phosphate buffer solution (PBS), containing 5×10^7 CFU/mL, on the plates with Sabouraud Dextrose Agar. The cultures were exposed to the plasma (17 W, 1.9 L/min) from a distance of 5 mm at different times with durations of 1 to 12 min. Then the plates were incubated at 35°C for 24 h. The growth inhibition zones induced by the plasma were elliptically shaped, where the major axis coincided with the parallel setting of the plasma beam (Fig. 9). Their size (assumed as half of the minor axis, c_{max}) was determined from photographs of the plates by densitometric analysis performed with Scion Image for Windows Alpha 4.0.3.2 (Scion Corporation, Frederick, Maryland, USA). The zone edge was defined as the location where cell viability reached 10% of survival in the nontreated plasma region. Each measurement was repeated five times and the result was averaged. The measurement error did not exceed 5%.

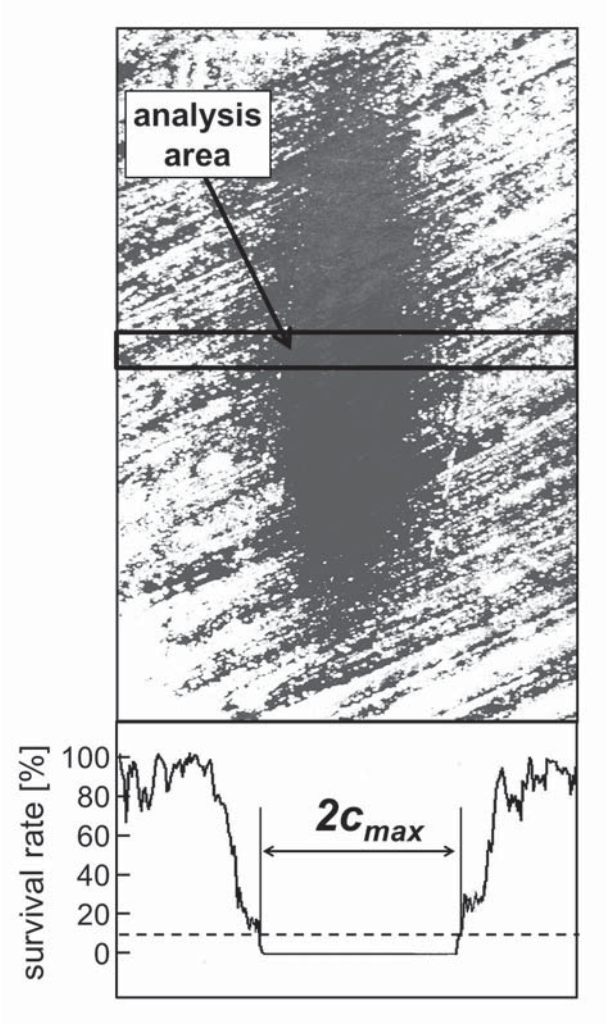

FIG. 9: Example of densitometric analysis determining inhibition zone growth under influence of plasma from razor jet (for *Prototheca zopfii*)

B. Results

Figure 10 shows an example of the survival rate of *C. albicans* cells as a function of discharge power and helium flow rate, measured after the first plasma treatment. As one can see, the increase in discharge power, regardless of the helium flow rate, decreases the number of living cells. This is understandable: with increasing discharge power, the density of the killing agents in the plasma increases. In turn, increasing the helium flow rate results in an increase in cell survival, which is a more complicated problem that is associated with reduced diffusion of oxygen and nitrogen, the main sources of killing agents, into the plasma area. Reduced oxygen and nitrogen interdiffusion with increas-

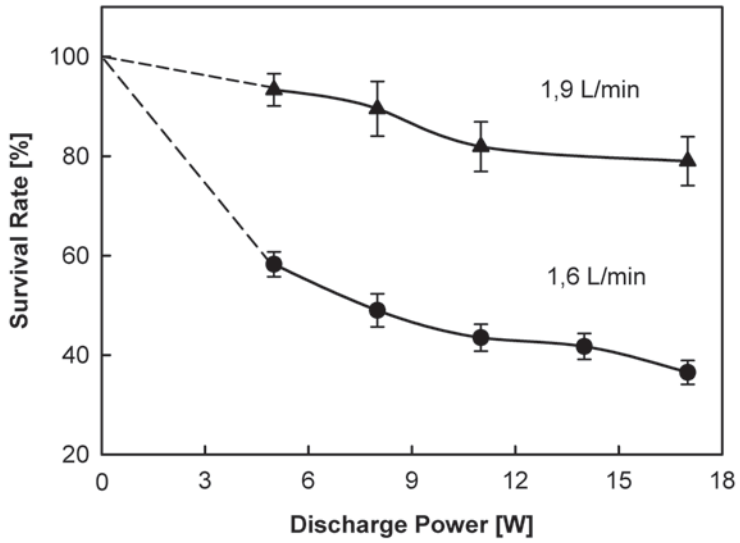

FIG. 10: Effect of discharge power and helium flow rate on survival of *Candida albicans* cells

ing helium flow rates was demonstrated in plasma emission spectroscopy studies (Fig. 4). However, it is important that a very short duration of treatment by the plasma razor jet is sufficient to produce a significant reduction in the survival of *C. albicans* cells.

Referring to clinical microbiological diagnostics, growth inhibition zones for the pathogenic fungi were tested using the second plasma treatment procedure. Examples of the dependence between of inhibition zone size (parameter c_{max} in Fig. 9) on plasma treatment time are shown for *C. albicans* and *P. zopfii* in Figs. 11 and 12, respectively. In the quantitative analysis of cold plasma cell killing, it was assumed that the edge of the growth inhibition zone corresponds to the minimal lethal dose (D_{min}) of the agents responsible for killing 90% of the cell population (a parameter analogous to minimum inhibitory concentration [MIC] in susceptibility tests). The minimal lethal dose can be expressed as

$$D_{\min} = E \cdot t \tag{3}$$

where t is the treatment time, and E is the irradiance at a point on the edge of the growth inhibition zone at a distance c_{max} from the zone's center (Fig. 9), interpreted as the number of killing agents per unit area and unit time reaching that point. Taking Eq. (2) and assuming that $h = ½ L$, we obtain the following relation:

$$D_{\min} = \frac{S_R L d^2 t}{(d^2 + c_{\max}{}^2)^{3/2} \left(d^2 + L^2/4\right)^{1/2}} \tag{4}$$

which, after transformation, gives the equation describing the dependence of the inhibition zone size on plasma treatment time:

$$c_{\max} = \left(\frac{t^{2/3}}{A} - d^2\right)^{1/2} \tag{5}$$

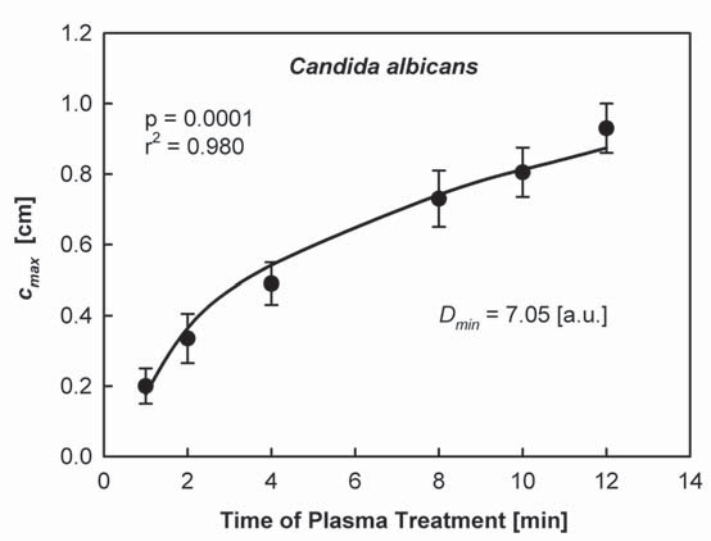

FIG. 11: Dependence of size of inhibition zone of *Candida albicans* growth on plasma treatment time (black points). Curve represents fit of experimental points with Eq. (5)

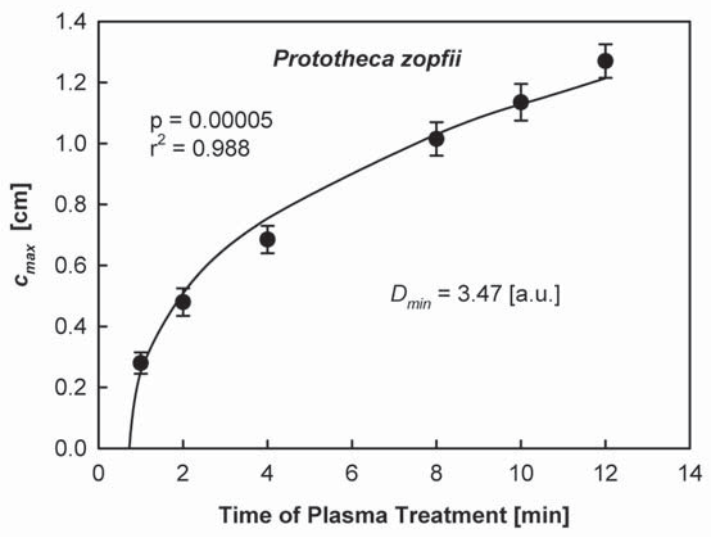

FIG. 12: Dependence of size of inhibition zone of *Prototheca zopfii* growth on plasma treatment time (black points). Curve represents fit of the experimental points with Eq. (5)

where

$$A = \left[\frac{D_{\min}\left(d^2+L^2/4\right)^{1/2}}{S_R L d^2}\right]^{2/3} \quad (6)$$

Equation (5) was used to describe the experimental data presented in Figs. 11 and 12. This fitting was carried out using TableCurve 1.12 (Jandel Scientific, San Rafael, CA). A very good adjustment of the curves calculated in Eq. (5) to experimental points was obtained for both *C. albicans* ($p = 0.0001$, $r^2 = 0.980$) and *P. zoffi* ($p = 0.00005$, $r^2 = 0.988$). As a result of the fitting, the factor A was determined, allowing D_{min} to be calculated. Assuming that $S_R = 1$, it was equal to 7.05 and 3.47 (a.u.) for the tested *C. albicans* and *P. zoffi* strains, respectively. In view of the above, *P. zopfii* is considerably more sensitive to the plasma treatment than *C. albicans*, despite the fact that *P. zopfii* strains are much more resistant than *C. albicans* to antifungal drugs.[30] This indicates a mechanism of plasma action on these microorganisms that is completely different from the mechanisms of action of conventional antifungal agents. This problem requires further extensive research.

IV. CONCLUSIONS

In this paper we have shown that cold plasma generated by a linear plasma device, the plasma razor jet, is well suited to surface treatment, providing sufficiently uniform irradiation during scanning. Such treatment is especially useful for all thermally unstable surfaces. Temperature changes on treated surfaces do not exceed several degrees for typical plasma razor jet operating parameters.

Our research on pathogenic fungi has shown the high effectiveness of linear cold plasma in killing fungal microorganisms. It takes only a few seconds of plasma action to significantly reduce the survival of the fungal cells. By analogy to clinical microbiology, where the MIC parameter is widely used, we have attempted to standardize our results by introducing the concept of minimal lethal dose (D_{min}), which has been theoretically defined and associated with the geometry of the plasma source. In this way, we can derive a formula describing D_{min} for other plasma sources, which will make it possible to compare their mechanisms of action on microorganisms.

REFERENCES

1. Friedman A, Friedman G. Plasma medicine. Chichester (UK): John Wiley & Sons; 2013.
2. Laroussi M, Kong MG, Morfill G, Stolz W, editors. Plasma medicine. Applications of low-temperature gas plasmas in medicine and biology. Cambridge (UK): Cambridge University Press; 2012.
3. Shintani H, Sakudo A, editors. Theory, applications, pitfalls and new perspectives. Gas plasma sterilization in microbiology. Norfolk (UK): Caister Academic Press; 2016.
4. Foest R, Schmidt M, Becker K. Microplasmas, an emerging field of low-temperature plasma science and technology. Int J Mass Spectrom. 2006;248:87–102.

5. Laroussi M, Tendero C, Lu X, Alla S, Hynes WL. Inactivation of bacteria by the plasma pencil. Plasma Process Polym. 2006;6:470–73.
6. Kolb JF, Mohamed A-AH, Price RO, Swanson RJ, Bowman A, Chiavarini RL, Stacey M, Schoenbach KH. Cold atmospheric pressure air plasma jet for medical applications. Appl Phys Lett. 2008;92(24):241501–3.
7. Kong MG, Kroesen G, Morfill G, Nosenko T, Shimizu T, van Dijk J, Zimermann JL. Plasma medicine: an introductory review. New J Phys. 2009;11:115012.
8. Chakravarthy K, Dobrynin D, Fridman G, Friedman G, Murthy S, Fridman A. Cold spark discharge plasma treatment of inflammatory bowel disease in an animal model of ulcerative colitis. Plasma Med. 2011;1(1):3–19.
9. Isbary G, Shimizu T, Li YF, Stolz W, Thomas HM, Morfill GE, Zimmermann JL. Cold atmospheric plasma devices for medical issues. Expert Rev Med Devices. 2013;10(3):367–77.
10. Setsuhara Y. Low-temperature atmospheric-pressure plasma sources for plasma medicine. Arch Biochem Biophys. 2016;605:3–10.
11. Nie QY, Cao Z, Ren CS, Wang DZ, Kong MG. A two-dimensional cold atmospheric plasma jet array for uniform treatment of large-area surfaces for plasma medicine. New J Phys. 2009;11:115015.
12. Hong YC, Shin DH, Lee SC, Uhm HS. Generation of large-volume plasma by making use of multi-needle plasma at low-pressure. Thin Solid Films. 2006;506–507:474–8.
13. Lee ES, Park HI, Baik HK, Lee SJ, Song KM, Hwang MK, Huh CS. Multi-jet atmospheric glow plasma cleaning of ablation debris from micro-via drilling process. Surf Coat Technol. 2003;171(1–3):307–11.
14. Moon SY, Han JW, Choe W. Feasibility study of material surface treatment using an atmospheric large-area glow plasma. Thin Solid Films. 2006;506–507:355–9.
15. Rhee JK, Kim DB, Moon SY, Choe W. Change of the argon-based atmospheric pressure large area plasma characteristics by the helium and oxygen gas mixing. Thin Solid Films. 2007;515(12):4909–12.
16. Kang JG, Kim HS, Ahn SW, Uhm HS. Development of the RF plasma source at atmospheric pressure. Surf Coat Technol. 2003;171:144–8.
17. Terajima T, Koinuma H. Development of a combinatorial atmospheric pressure cold plasma processor. Appl Surf Sci. 2004;223(1–3):259–63.
18. Lee ES, Choi JH, Baik HK. Surface cleaning of indium tin oxide by atmospheric air plasma treatment with the steady-state airflow for organic light emitting diodes. Surf Coat Technol. 2007;201:4973–78.
19. Baránková H, Bardosab L. Hollow cathode and hybrid plasma processing. Vacuum. 2006;80:688–92.
20. Schlemm H, Roth D. Atmospheric pressure plasma processing with microstructure electrodes and microplanar reactors. Surf Coat Technol. 2001;142–144:272–6.
21. Kazimierski P, Tyczkowski J, Zieliński J, inventors. Microplasma electrode reactor for the surface treatment under atmospheric pressure. Polish patent PL212569. 2012 Dec 2.
22. Rezaei F, Dickey MD, Bourham M, Hauser PJ. Surface modification of PET film via a large area atmospheric pressure plasma: an optical analysis of the plasma and surface characterization of the polymer film. Surf Coat Technol. 2017;309:371–81.
23. Kramida A, Ralchenko Y, Reader J; NIST ASD Team. NIST Atomic Spectra Database (version 5.4) [database on the Internet]. Gaithersburg (MD): National Institute of Standards and Technology, c2017 [cited 2017 Sep 20]. Available from: http://physics.nist.gov/asd.
24. Ocean Optics Mikropack. SpecLine Offline Spectroscopy Analysis Software. Version 2.13 [software], Ostfildern (GER): Ocean Optics Mikropack; 2004.
25. Laroussi M, Leipold F. Evaluation of the roles of reactive species, heat, and UV radiation in the inactivation of bacterial cells by air plasmas at atmospheric pressure. Int J Mass Spectrom. 2004;233(1–3):81–6.
26. Cullen PJ, Milosavljević V. Spectroscopic characterization of a radio-frequency argon plasma jet discharge in ambient air. Prog Theor Exp Phys. 2015;063J01:1–17.
27. Ryder A. The light measurement handbook. Newbury (MA): International Light Technical Publications; 1997.

28. Akehata T, Shirai T. Effect of light-source characteristics on the performance of circular annular photochemical reactor. J Chem Eng Japan. 1972;5:385–91.
29. Grimes DR, Robbins C, O'Hare NJ. Dose modeling in ultraviolet phototherapy. Med Phys. 2010; 37:5251–57.
30. Tyczkowska-Sieron E, Markiewicz J, Grzesiak B, Krukowski H, Glowacka A, Tyczkowski J. Cold atmospheric plasma inactivation of Prototheca zopfii isolated from bovine milk. J Dairy Sci. 2018;101:118–22.